Femtosecond dynamics of excited states of CO adsorbed on MgO(001)-(1×1)

Neng-Ping Wang,[1] Michael Rohlfing,[1] Peter Krüger,[2] and Johannes Pollmann[2]
[1]*School of Engineering and Science, International University Bremen, P.O. Box 750561, 28725 Bremen, Germany*
[2]*Institut für Festkörpertheorie, Universität Münster, 48149 Münster, Germany*
(Received 18 June 2004; revised manuscript received 29 October 2004; published 11 January 2005)

We have investigated the time development of excited electronic states of CO molecules adsorbed on the MgO(001)–(1×1) surface using a state-of-the-art first principles approach. Density-functional theory is used to calculate the ground state geometry of the clean surface and of the molecules adsorbed on the surface. Thereafter, the quasiparticle band structures of bulk MgO, of the MgO(001)–(1×1) surface, and of CO adsorbed on the surface are calculated within the *GW* approximation. Taking the electron-hole interaction into consideration the electron-hole excitations and their optical spectrum are obtained from the solution of the Bethe-Salpeter equation for the electron-hole two-particle Green function. The optical spectra of bulk MgO, the MgO(001)–(1×1) surface, and CO adsorbed on the surface are calculated, yielding good agreement with available experimental data. Finally, based on the solution of the BSE for the adsorbate system CO:MgO(001)–(1×1), the time propagation of molecular excitations is studied employing the time-dependent Schrödinger equation. An initial CO excitation exhibits a very fast decay due to its coupling to charge-transfer exciton states between the substrate and the adsorbate. The decay is characterized by a lifetime of about 1.6 fs, which is a factor of 5 faster than the decay of single-particle states.

DOI: 10.1103/PhysRevB.71.045407 PACS number(s): 73.20.Hb, 34.50.Gb, 34.70.+e, 82.53.Xa

I. INTRODUCTION

Dynamical properties of excited electronic states have recently received a great deal of attention due to their fundamental importance in physics and chemistry.[1–4] In this context the adsorbate–substrate interaction between molecules and crystal surfaces is of particular interest.[1–4] Such interaction has widely been discussed regarding electronic ground-state properties, like scattering, catalysis, and crystal growth. It is of equally high importance for excited states since it plays a crucial role for fast electronic processes encountered in short time spectroscopy, photochemistry, or excitation-induced desorption. An example of excited-state dynamics is the transfer of localized excitations to other positions in space due to energetic resonance. For instance, electrons or holes excited on an adsorbate may transfer into the substrate, which often causes a fast decay of the particle amplitude on the adsorbate.[5] The decay of single-particle states has been studied for atoms and molecules on metal surfaces and on semiconductors.[6–8] The strong bonds between the chemically active substrate and the adsorbate account for the decay processes of single-particle states. Insulator substrates, on the other hand, are often chemically inert and their electronic levels are off-resonant with those of the adsorbate. This constitutes a barrier for charge-carrier hopping and limits the possibilty of decay. However, we find that such a barrier for adsorbate-state decay can be completely absent for two-particle states (in particular, for excitons) even if hopping of single particles is prohibited. As a prototype case, we investigate the decay of molecular excitations of CO adsorbed on MgO(001)–(1×1) by investigating the real-time propagation of the states. Here we observe a very fast charge transfer process on a femtosecond time scale.[9]

For the electronic ground state of many-particle systems, density-functional theory (DFT) has proven to be a powerful tool. Accurate results for the ground-state geometry of the system and electronic one-particle wave functions can be obtained from this theory. Excited electronic states like quasiparticle (QP) excitations and correlated electron-hole excitations, however, are in general not directly accessible in a DFT calculation. The state-of-the-art approach to QP excitations is Hedin's approximation (GWA),[10,11] in which the nonlocal, energy-dependent electron self-energy is given by a convolution of the one-electron Green function and the dynamically screened Couloumb interaction. Very accurate quasiparticle properties have been obtained by this method.[12] Optical excitations of semiconductors and insulators are dominated by electron-hole correlation effects which are not described by the independent-quasiparticle image. It has been found that the accurate calculation of optical excitations requires an effective two-body approach, which must take the electron-hole interaction into consideration.[13–17] A rigorous approach to optical spectra is the two-body Green function method.[18] The solution of the equation of motion for the two-body Green function (the Bethe-Salpeter equation) yields coupled excited electron-hole states from which the optical absorption spectrum can be evaluated. This approach has been applied to investigate bulk crystals, polymers, and gas-phase molecules,[14–17,19,20] as well as nonconducting-solid surfaces,[21–24] yielding very accurate results.

The adsorption of the CO molecule on ionic surfaces, like magnesium oxide (MgO), is of continuous interest in theory[25–29] and experiment.[30,31] On the theoretical side, the adsorption geometries, adsorption energies, and C–O vibration frequencies are thoroughly studied. However, much less information is available on the time evolution of excited electronic states of CO on MgO, so far. In this paper, we present in detail an *ab initio* calculation of time-dependent dynamics of excited electronic states of CO adsorbed on the MgO(001)–(1×1) surface, where we have recently observed a very fast charge-transfer process.[10] In particular, we com-

pare the dynamical properties of single-particle states (electrons or holes, respectively) with the decay of a correlated electron-hole pair excitation. The latter turns out to have a much shorter lifetime on the molecule than the single-particle states. The reason for this behavior, which relies on the interplay between band-structure energies and electron-hole attraction, is analyzed and visualized in terms of the wave functions of the respective states. A systematic comparison of various systems [i.e., the clean MgO(001)–(1×1) surface, a free-standing monolayer of CO molecules without the MgO substrate, and the coupled substrate-adsorbate system] is used to reveal the details of the underlying mechanism of decay and charge transport.[9]

The paper is organized as follows. In Sec. II, we briefly summarize the basic theoretic formalism. In Sec. III, we discuss optical excitations of the MgO bulk crystal, and we calculate the ground-state geometry of the MgO(001)–(1×1) surface, the corresponding band structure, and the optical absorption spectrum, thus preparing the basis for discussing the adsorbate system. In Sec. IV, we investigate the adsorption of CO on MgO(001)–(1×1), as well as the band structure and excitation spectrum of CO:MgO(001)–(1×1). In Sec. V we discuss the time evolution of excited one-particle states and of electron-hole pair excitations of the CO molecule when the molecule is coupled to the substrate. A short summary concludes the paper in Sec. VI.

II. BASIC THEORETICAL FORMALISM

A. Electronic ground state

The ground-state properties of molecules and crystals can be described within density-functional theory (DFT) using the local-density approximation (LDA). The resulting Kohn-Sham equation is given by

$$\left\{-\frac{\hbar^2}{2m}\nabla^2+V_{ps}(\mathbf{r})+V_H(\mathbf{r})+V_{xc}(\mathbf{r})\right\}\psi_{n\mathbf{k}}^{\mathrm{LDA}}(\mathbf{r}) = E_{n\mathbf{k}}^{\mathrm{LDA}}\psi_{n\mathbf{k}}^{\mathrm{LDA}}(\mathbf{r}), \tag{1}$$

where V_{ps} and V_H are the potential of the ions and the Hartree potential, respectively. Nonlocal, norm-conserving *ab initio* pseudopotentials are used in the present work. The potential for Mg was provided by Fritsch,[32] and the potentials for C and O are given by Bachelet *et al.*[33] Solving Eq. (1) self-consistently yields the LDA band structure, wave functions, total energy, and forces on the atoms, which we use to optimize the geometric structure.

Gaussian orbitals are used to construct the LDA basis sets.[34] We use 30 Gaussian orbitals of *s*, *p*, *d*, and s^* type for all Mg, O, and C atoms. The decay constants (in atomic units) are 0.2, 0.55, and 0.95 for Mg, 0.25, 1.0, and 3.7 for molecular and substrate O, and 0.15, 0.671, and 3.0 for C. Gaussian orbitals are also used as basis functions for the representation of all quantities occurring in the GW self-energy operator and the electron-hole interaction in the next section. A suitable choice of decay constants for these basis functions is given by 0.25 and 0.9 for Mg, 0.35, 1.2, and 4.0 for O, and 0.15, 0.671, and 3.0 for C.

B. Single-particle excitations: Electrons and holes

Quasiparticle excitations (electrons and holes) can be described using many-body perturbation theory,[10,11] in which the self-energy operator Σ is expanded in a series containing the one-body Green function G_1 and the screened Coulomb interaction W of the system. The first term of the expansion constitutes the GW approximation:[11,34,35]

$$\Sigma(\mathbf{r},\mathbf{r}',E)=\frac{i}{2\pi}\int e^{-i\omega 0^+}G_1(\mathbf{r},\mathbf{r}',E-\omega)W(\mathbf{r},\mathbf{r}',\omega)d\omega. \tag{2}$$

We approximate G_1 by the results of the DFT-LDA calculation. For the frequency dependence of W we employ a generalized plasmon-pole approximation. The static part $W(\omega=0)$ of the interaction is calculated using the random-phase approximation (RPA). After constructing the nonlocal, energy-dependent self-energy operator $\Sigma(\mathbf{r},\mathbf{r}',E)$, we solve the quasiparticle equation for periodic systems:[34]

$$\left\{-\frac{\hbar^2}{2m}\nabla^2+V_{ps}(\mathbf{r})+V_H(\mathbf{r})\right\}\psi_{n\mathbf{k}}^{\mathrm{QP}}(\mathbf{r}) + \int\Sigma(\mathbf{r},\mathbf{r}',E_{n\mathbf{k}}^{\mathrm{QP}})\psi_{n\mathbf{k}}^{\mathrm{QP}}(\mathbf{r}')d^3r' = E_{n\mathbf{k}}^{\mathrm{QP}}\psi_{n\mathbf{k}}^{\mathrm{QP}}(\mathbf{r}), \tag{3}$$

which differs from the Kohn-Sham equation by replacing V_{xc} by the self energy $\Sigma(E)$. This difference $[\Sigma(E)-V_{xc}]$ constitutes a QP correction to the LDA band structure. For semiconductors and insulators, this correction is often in the order of 1–10 eV. For the systems studied in this paper the LDA wave functions $|\psi_{n\mathbf{k}}^{\mathrm{LDA}}\rangle$ are already very close to $|\psi_{n\mathbf{k}}^{\mathrm{QP}}\rangle$. We thus consider QP corrections to the band-structure energies only, not to the wave functions.

C. Electron-hole excitations

While the GWA yields band structures in good agreement with experimental data for single-particle excitations, optical properties cannot be obtained correctly from QP band structures within an independent-particle picture. This is due to the interaction between the excited electron and hole occurring in optical excitations. To describe the resulting two-body correlation effects on optical properties, an effective two-particle theory is required. The most general procedure for calculating optical spectra is to consider the equation of motion of the two-body Green function G_2.[18] This procedure can be formulated in terms of coupled electron-hole excited states $|S_{\mathbf{Q}}\rangle$. We expand these states in a basis given by the QP states as[17]

$$|S_{\mathbf{Q}}\rangle=\sum_{\mathbf{k}}\sum_{v}^{\text{hole}}\sum_{c}^{\text{elec}}A_{vc\mathbf{k}}^{S\mathbf{Q}}|vc\mathbf{k}\rangle=\sum_{\mathbf{k}}\sum_{v}^{\text{hole}}\sum_{c}^{\text{elec}}A_{vc\mathbf{k}}^{S\mathbf{Q}}\hat{a}_{v\mathbf{k}}^{+}\hat{b}_{c,\mathbf{k}+\mathbf{Q}}^{+}|0\rangle, \tag{4}$$

where $\hat{a}_{v\mathbf{k}}^{+}$ and $\hat{b}_{c,\mathbf{k}+\mathbf{Q}}^{+}$ denote the operators creating a hole (in valence band v at wave vector $\mathbf{k}$) and an electron (in conduction band c at wave vector $\mathbf{k}+\mathbf{Q}$), respectively, in the many-body ground state $|0\rangle$. $\mathbf{Q}$ is the total momentum of the

electron-hole state which, in optical processes, corresponds to the momentum of the involved photon. Since the photon wavelength is very large compared to the lattice constant of crystals, the momentum **Q** of the exciton created in photoabsorption is very close to zero. Nevertheless, the direction of the exciton momentum **Q** may be important for details of the spectrum. For shortness sake, we suppress the index **Q** at S in the following equations.

Since the electronic ground states of all systems studied here [MgO, MgO(001)–(1×1), CO, and CO:MgO(001)–(1×1)] are given by closed-shell spin-singlet states, the excitations can be classified (in the absence of spin–orbit interaction) as singlet-to-singlet and singlet-to-triplet excitations. We focus on the singlet-to-singlet transitions that are relevant for the optical spectra. From the equation of motion of G_2, one obtains the Bethe-Salpeter equation (BSE) of the excited states $|S\rangle$:[17,18]

$$(E^{\mathrm{QP}}_{c,\mathbf{k}+\mathbf{Q}}-E^{\mathrm{QP}}_{v,\mathbf{k}})A^S_{vc\mathbf{k}}+\sum_{\mathbf{k}'}\sum_{v'}^{\text{hole}}\sum_{c'}^{\text{elec}}\langle vc\mathbf{k}|K^{eh}|v'c'\mathbf{k}'\rangle A^S_{v'c'\mathbf{k}'} = \Omega_S A^S_{vc\mathbf{k}}. \tag{5}$$

Equation (5) can be interpreted as the eigenequation of an effective two-particle Hamiltonian for correlated electron-hole states, which is defined as $H^{eh}_{vc\mathbf{k},v'c'\mathbf{k}'}=(E^{\mathrm{QP}}_{c,\mathbf{k}+\mathbf{Q}}-E^{\mathrm{QP}}_{v,\mathbf{k}})\delta_{v,v'}\delta_{c,c'}\delta_{\mathbf{k},\mathbf{k}'}+\langle vc\mathbf{k}|K^{eh}|v'c'\mathbf{k}'\rangle$. The electron-hole interaction K^{eh} is given by

$$\langle vc\mathbf{k}|K^{eh}|v'c'\mathbf{k}'\rangle = -\int d\mathbf{r}d\mathbf{r}'\,\psi^*_{c,\mathbf{k}+\mathbf{Q}}(\mathbf{r})\psi_{c',\mathbf{k}'+\mathbf{Q}}(\mathbf{r})W(\mathbf{r},\mathbf{r}')\psi_{v\mathbf{k}}(\mathbf{r}')\psi^*_{v'\mathbf{k}'}(\mathbf{r}') + 2\cdot\int d\mathbf{r}d\mathbf{r}'\,\psi^*_{c,\mathbf{k}+\mathbf{Q}}(\mathbf{r})\psi_{v\mathbf{k}}(\mathbf{r})v(\mathbf{r},\mathbf{r}')\psi_{c',\mathbf{k}'+\mathbf{Q}}(\mathbf{r}')\psi^*_{v'\mathbf{k}'}(\mathbf{r}'). \tag{6}$$

The first term of Eq. (6) is a screened, direct electron-hole interaction term. We evaluate this from the static dielectric matrix, neglecting dynamical effects.[18] This is justified because the exciton binding energies are small in comparison to the band gap, which defines the characteristic energy scale of the dynamics of the dielectric screening. The second term of Eq. (6) is an exchange interaction term, which describes the short-range part of the bare Coulomb interaction. The factor of 2 in this term results from the spin degrees of freedom of the singlet-to-singlet excitations studied here.

Once the Bethe-Salpeter Eq. (5) is solved, the obtained coefficients $A^S_{vc\mathbf{k}}$ can be used to evaluate the real-space wave function of an excited state $|S\rangle$,

$$\Psi_S(\mathbf{r}_e,\mathbf{r}_h)=\sum_{\mathbf{k}}\sum_{v}^{\text{hole}}\sum_{c}^{\text{elec}}A^S_{vc\mathbf{k}}\psi^*_{v\mathbf{k}}(\mathbf{r}_h)\psi_{c\mathbf{k}+Q}(\mathbf{r}_e), \tag{7}$$

where $\mathbf{r}_e$ and $\mathbf{r}_h$ denote the coordinates of the electron and hole, respectively. Furthermore, the entirety of all excited states yields the optical spectrum. In particular, the imaginary part of the macroscopic transverse dielectric function, for instance, is given by[17]

$$\epsilon_2(\omega)=\frac{16\pi^2e^2}{\omega^2}\sum_S\left|\sum_{\mathbf{k}}\sum_{v}^{\text{hole}}\sum_{c}^{\text{elec}}A^S_{vc\mathbf{k}}\langle v\mathbf{k}|\boldsymbol{\lambda}\cdot\mathbf{v}|c\mathbf{k}\rangle\right|^2 \times\delta(\omega-\Omega_S), \tag{8}$$

where $\boldsymbol{\lambda}$ is the polarization vector of the light and $\mathbf{v}=i[H^{sp},\mathbf{r}]/\hbar$ is the single-particle velocity operator (which corresponds to the current operator). Here H^{sp} denotes the single-particle Hamiltonian.

D. Time-dependent dynamics of electronic excitations

In Sec. V we will consider the time-dependent Schrödinger equation,

$$i\hbar\frac{\partial}{\partial t}|\Psi(t)\rangle=H^{eh}|\Psi(t)\rangle,$$

for an electron-hole excited-state wave function $|\Psi(t)\rangle$ of the adsorbate system of CO on MgO. H^{eh} denotes the effective two-particle Hamiltonian of Eq. (5) of the substrate–adsorbate system. In all cases discussed in this paper, we will define an initial state, $|\Psi(t=0)\rangle$, which is usually given by an eigenstate of the molecule on its own. Taking the coupling to the MgO substrate into account (which is automatically included in the Hamiltonian H^{eh}), $|\Psi(t=0)\rangle$ is no longer an eigenstate of the coupled substrate–adsorbate system and will exhibit time propagation. This time propagation of $|\Psi(t)\rangle$ can be investigated by directly integrating the Schrödinger equation.[22] Alternatively, it can also be calculated by expanding $|\Psi(t=0)\rangle$ in all the eigenstates of the Hamiltonian. If the initial exciton state is mapped onto all eigenstates of the Hamiltonian, one obtains

$$|\Psi(t=0)\rangle=\sum_S\langle S|\Psi(t=0)\rangle|S\rangle. \tag{9}$$

Since H^{eh} is not explicitly time dependent, the solution of the time-dependent Schrödinger equation is simply given by

$$|\Psi(t)\rangle=\exp\left(-\frac{i}{\hbar}H^{eh}t\right)|\Psi(t=0)\rangle. \tag{10}$$

Substituting Eq. (9) into Eq. (10) and noticing that $H^{eh}|S\rangle=\Omega_S|S\rangle$, $|\Psi(t)\rangle$ is given by

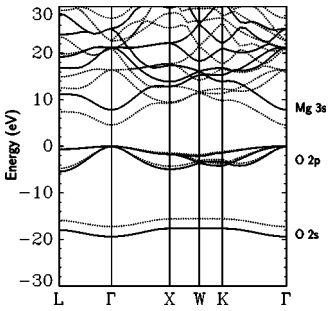

FIG. 1. Bulk band structure of MgO, as obtained within GWA (solid curves) and within LDA (dotted curves).

$$|\Psi(t)\rangle = \sum_S \langle S|\Psi(t=0)\rangle \exp\left(-\frac{i}{\hbar}\Omega_S t\right)|S\rangle, \qquad (11)$$

where Ω_S is an eigenvalue of the two-particle Hamiltonian determined by Eq. (5). Since we evaluate the eigenstates $|S\rangle$ anyway (for analysis and comparison purposes), the expansion of $|\Psi(t)\rangle$ is obtained immediately. If one were just interested in $|\Psi(t)\rangle$ only, real-time integration of the Schrödinger equation as an ordinary differential equation in t would be more economic, thus avoiding diagonalization of the Hamiltonian.

From Eqs. (7) and (11) it follows that the two-particle real-space wave function of $|\Psi(t)\rangle$ is given by

$$\Psi(\mathbf{r}_e,\mathbf{r}_h,t) = \sum_{\mathbf{k},v,c} \left\{ \sum_S A^S_{vc\mathbf{k}} \langle S|\Psi(t=0)\rangle \times \exp\left(-\frac{i}{\hbar}\Omega_S t\right) \right\} \psi^*_{v\mathbf{k}}(\mathbf{r}_h)\psi_{c\mathbf{k}+\mathbf{Q}}(\mathbf{r}_e). \qquad (12)$$

The approach discussed here can also be used to calculate the time evolution of a *single* particle state $|\psi_{\mathbf{k}}(t)\rangle$ at wave vector $\mathbf{k}$. For this case, we get

$$|\psi_{\mathbf{k}}(t)\rangle = \sum_n \langle \psi^{\mathrm{QP}}_{n\mathbf{k}}|\psi_{\mathbf{k}}(t=0)\rangle \exp\left(-\frac{i}{\hbar}E^{\mathrm{QP}}_{n\mathbf{k}}t\right)|\psi^{\mathrm{QP}}_{n\mathbf{k}}\rangle. \qquad (13)$$

III. ELECTRONIC EXCITATIONS OF THE MgO BULK CRYSTAL AND OF THE MgO(001)–(1×1) SURFACE

In this section some basic results concerning the geometric and electronic structure of MgO and its (001) surface are briefly summarized to provide the basis of Secs. IV and V. For further details we refer to Ref. 36.

A. MgO bulk crystal

MgO is an ionic insulator with rocksalt structure, having a lattice constant of $a=4.21$ Å. Figure 1 shows the MgO bulk band structure, calculated within GWA (solid lines) and LDA (dashed lines).

The GW valence band structure consists of four bands, i.e., one O 2*s* band (at about −18.6 eV) and three O 2*p* bands (between −5.5 and 0 eV). We label the lowest conduction band as Mg 3*s*, although this classification is not exactly possible due to significant coupling of the Mg 3*s* orbital to other states. The band gap amounts to 4.53 eV within LDA and 7.79 eV within GWA. The latter is in very good agreement with the experimental value of 7.83 eV.[37]

Using the approach presented in Sec. II C, the optical spectrum can be calculated. Particular attention has to be paid to the number of valence bands, conduction bands, and **k** points for the expansion of the excited states [cf. Eq. (4)], both for the bulk crystal and for the surface systems (see Sec. III B). All data are compiled in Table I.

Initially, we have included the three O 2*p* valence bands ($v=2$–4) and the four lowest conduction bands ($c=5$–8), yielding good convergence of all excitations below about 20 eV. We use 256 **k** points (i.e., an equidistant grid of spacing $1/8\times 2\pi/a$, yielding 512 **k** points in a cube of side length $2\pi/a$, of which 256 **k** points are inside the Brillouin zone of the fcc structure), yielding a resolution of better than ~0.2 eV in the continuous part of the resulting spectrum. Figure 2 compares the resulting ϵ_2 spectrum (solid line) with experiment.[38]

Good agreement between experiment and theory is obtained, with the peak positions being well reproduced. The

TABLE I. Number of valence bands (N_V), conduction bands (N_c), and **k** points ($N_{\mathbf{k}}$) used in the BSE calculations for the various systems discussed in this paper. All surface systems are in the (001)–(1×1) geometry.

System	N_v	N_c	$N_{\mathbf{k}}$	Dim.	Remarks
(1) MgO bulk	3	4	1/2 of 8×8×8=256	3072	Converged
(2) MgO bulk	3	1	1/2 of 8×8×8=256	768	Exciton well represented
(3) MgO surf., six layers	18	24	6×6=36	15552	Consistent with 1.
(4) MgO surf., six layers	18	6	6×6=36	3888	Consistent with 2.
(5) CO monolayer	4	3	6×6=36	432	Converged $\|^1\Pi\rangle$ state
(6) CO:MgO, six layers	4+18	3+6	6×6=36	7128	Consistent with 4./5.
(7) CO:MgO, four layers	4+12	3+4	6×6=36	4032	Convergence test
(8) CO:MgO, seven layers	4+21	3+7	6×6=36	9000	Convergence test
(9) CO:MgO, four layers	4+12	3+4	8×8=64	7168	Convergence test
(10) CO:MgO, four layers	4+12	3+4	10×10=100	11200	Convergence test

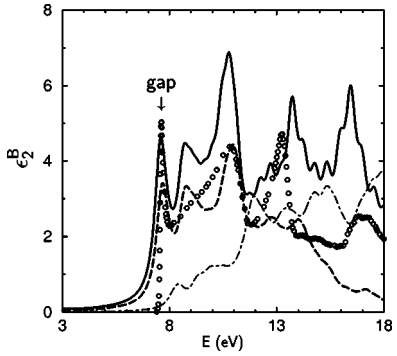

FIG. 2. Optical absorption spectrum $\epsilon_2^B(\omega)$ of bulk MgO, calculated from three valence and four conduction bands (solid curve), as well as from three valence and one conduction bands (dashed curve), respectively. The dash–dotted curve shows the independent-particle spectrum, i.e., without including the electron–hole interaction. A Lorentzian broadening of 0.3 eV has been used. The open circles denote the experimental result taken from Ref. 38.

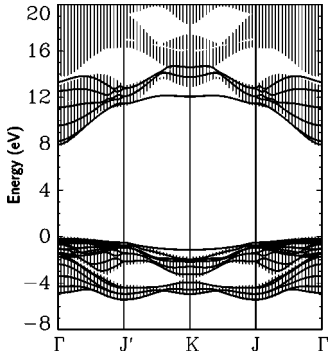

FIG. 3. Surface band structure of MgO(001)–(1×1), obtained within GWA. Only the bands that are included in the Bethe-Salpeter equation are shown. The vertical lines indicate the projected bulk band structure.

first exciton peak is located at 7.7 eV with very small binding energy (0.1 eV). To see the effect of the electron–hole interaction, the optical spectrum obtained from GWA interband transitions only (without electron–hole interaction) is plotted as the dot-dashed curve in Fig. 2, as well. Apparently, the entire spectrum is significantly affected by the electron–hole interaction, as expected for a system with weak screening. Our results are essentially the same as those obtained by Benedict *et al.* in a similar calculation.[15]

The main contributions to the low-energy excitations stem from transitions into the lowest conduction band (Mg 3*s*). It is thus sufficient to restrict the expansion of Eq. (4) to transitions from O 2*p* to Mg 3*s*, only (see Table I) when focusing on the low-energy part of the spectrum. The resulting spectrum for bulk MgO is shown by the dashed line in Fig. 2. Apparently, for energies below 12 eV this spectrum is in good agreement with the fully converged spectrum, with the peak positions being reproduced very well. Note, however, that the amplitude of the spectrum is significantly affected due to missing optical dipole contributions from the higher conduction bands. In the case of the MgO(001)–(1×1) surface and of the CO:MgO(001)–(1×1) adsorbate system this means that, as long as we are mainly interested in the energetic positions of low-energy exciton states i.e., below 12 eV, it will be sufficient to restrict the number of contributing empty substrate bands to one band per Mg atom in the unit cell.

B. MgO(001)–(1×1) surface

The MgO(001)–(1×1) surface does not reconstruct and exhibits weak relaxations, only ($\delta z=-0.03$ Å for the surface Mg atoms and $\delta z=0.03$ Å for the surface O atoms). We represent the surface system by a supercell geometry of six atomic layers (6 Mg atoms and six O atoms) and a vacuum layer of 12.7 Å. Figure 3 shows the corresponding GWA band structure.

While most of the states are bulk-like, only the highest valence bands and the lowest conduction bands (near the *K* point) are truly localized surface states. As expected for an ionic system without chemically active dangling-bond surface states, the QP corrections at the surface are very similar to those in the bulk.

Since the surface is represented by six atomic layers (six Mg atoms and six O atoms), $6\times$ as many valence and conduction bands have to be taken into account for the optical excitations to be consistent with the bulk calculations (Table I). The case of three valence and four conduction bands in the bulk calculation of the ϵ_2 spectrum would then translate to 18 valence and 24 conduction bands in the slab representing the surface. This quadratic scaling with system size leads to matrices in Eq. (5) that are too demanding to diagonalize (see Table I). Fortunately, as discussed in Sec. III A, we can reduce the size of the matrix in Eq. (5) by considering one conduction band per Mg atom, only (i.e., six conduction bands in total), yielding accurate excited-state data below about 12 eV excitation energy. (When the CO monolayer is adsorbed, three more conduction bands will be included to account for the molecule states.)

Figure 4 shows the optical absorption spectrum of MgO(001)–(1×1) for normal incidence. The spectrum is dominated by a strong peak below the QP surface band gap ($E_{\mathrm{gap}}^{\mathrm{surf}}=8.1$ eV).

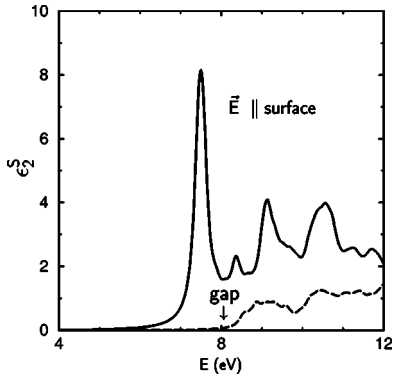

FIG. 4. Optical absorption spectrum of the MgO(001)–(1×1) surface (calculated for normal incidence of light) is shown as solid curve. For comparison the independent-particle spectrum, calculated without electron–hole interaction, is shown as a dashed curve. Lorentzian broadening of 0.14 eV is included.

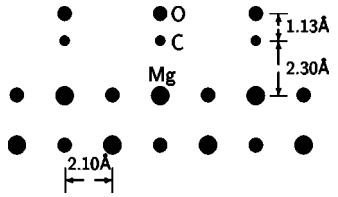

FIG. 5. Optimal adsorption geometry of CO on MgO(001)–(1 $\times$1) (side view). Note that the figure shows a plane ([100] plane of the underlying MgO bulk crystal) in which second-nearest-neighbor CO molecules are displayed (at a distance of 4.21 Å).

This peak originates from four states that are degenerate in energy. The detailed analysis of their wave functions shows that these states are strongly localized at the surface, i.e., they are surface excitons. The binding energy of the lowest exciton is 0.6 eV, which is significantly stronger than the binding energy of the bulk exciton (0.1 eV). The wave functions of these states are similar to those presented in Ref. 23 for the LiF(001)–(1 $\times$ 1) surface. In the following section, these excited states will be coupled with the excitations of adsorbed CO molecules.

IV. EXCITED STATES OF CO:MgO(001)–(1×1)

Before addressing the electronic and optical excitations, the geometry of the adsorbate system CO:MgO(001)–(1 $\times$1) is considered first.

A. Geometry

We start from the previous (1 $\times$ 1) surface unit cell, which consists of six substrate layers. We consider the adsorption of one full monolayer, i.e., one CO molecule in each (1 $\times$ 1) surface unit cell (see Fig. 5). Minimum total energy is achieved for vertical adsorption with the molecule C atom bound to Mg (Mg–C–O). Tilted orientations and binding via substrate O atoms leads to higher energy, while binding via the O atom of the molecule is repulsive. The optimized geometry is shown in Fig. 5.

The C–O and C–Mg bond lengths result as 1.13 and 2.3 Å, respectively, in good agreement with earlier embedded-cluster calculations[25,27] and periodic DFT calculations.[26,28] The adsorption energy per unit cell amounts to 0.5 eV in LDA, which is close to the value of 0.3 eV per molecule given by a previous DFT-LDA calculation using the full-potential linearized augmented plane-wave (FLAPW) method.[26] Note that LDA usually yields good adsorption geometries but tends to overestimate adsorption energies. In the present case of CO:MgO(001)−(1 $\times$ 1), DFT calculations within the generalized gradient approximation (GGA) yield an adsorption energy of no more than 0.1 eV.[27,28] Experimental investigations have reported adsorption energies between 0.15 and 0.43 eV for a single CO molecule on MgO(001).[30,31]

B. Quasiparticle band structure

Figure 6 shows the GW quasiparticle band structure of CO:Mg(001)−(1 $\times$ 1).For comparison, the GW band structure of an isolated CO monolayer (i.e., the same system without the MgO substrate) is shown in the left panel. From analyzing the wave functions, the states of the combined system can clearly be identified as molecular states (displayed as solid lines) and MgO substrate states (dashed lines), respectively. Both in the isolated monolayer and in the adsorbate system, the CO bands show significant dispersion caused by intermolecular single-particle coupling of up to 1 eV due to the small distance of 2.98 Å between the molecules. A tight-binding analysis of this dispersion allows us to evaluate the single-particle levels of a single CO molecule on MgO. These are shown in the right-hand panel of Fig. 6, accompanied by a schematic representation of the MgO density-of-states. The CO states and the substrate states are separated in energy. The CO hole states (4σ at -18.4 eV, 1π at -15.3 eV, and 5σ at -13.4 eV) are located below the valence bands of MgO (from -13.2 to -7.4 eV). The CO electron state ($2\pi^*$ at 0.7 eV) is located near the MgO bulk conduction band minimum at 0.4 eV, i.e., it is located at an energy at which the density of states of the substrate is very small. There is very little interaction between the molecular states and the substrate states, leading to weak level repulsion. This implies that holes or electrons excited in the molecular orbitals should have a rather low probability of hopping to the substrate.

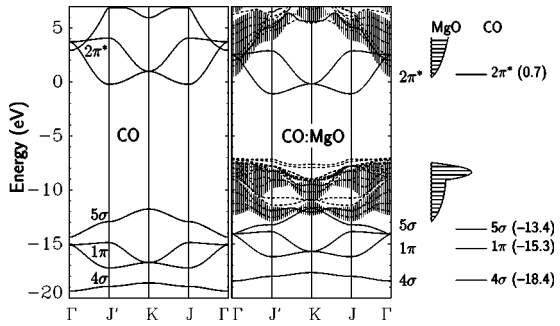

FIG. 6. Left panel: GW band structure of an isolated CO monolayer, center panel: GW band structure of CO:MgO(100)–(1 $\times$ 1), solid and dashed curves denote CO and MgO bands, respectively. The energies refer to the vacuum level [at VBM(MgO)+7.4 eV]. The vertical lines indicate the projected bulk band structure. Right panel: onsite energies of the CO bands of the center panel, as obtained by tight-binding analysis, indicating the energetic positions of a single CO molecule adsorbed on MgO. The numbers given in brackets denote the onsite energies, allowing the direct comparison with the energy levels of gas-phase CO.

It is interesting to note that the CO hole levels of the adsorbed molecule are higher in energy than those of a single CO molecule in the gas phase, while the electron level is lower than in the gas phase. For gas-phase CO we obtain energies of -19.4, -16.9, and -13.9 eV for 4σ, 1π, and 5σ, which are in very good agreement with measured ionization energies of -19.8, -17.0, and -14.0, respectively.[39] At the surface, these levels are raised by about 1 eV. (The 5σ level is raised by 0.5 eV, only, due to level repulsion from the MgO valence states.) The $2\pi^*$ level, on the other hand, which we find at 2.4 eV in the gas phase (as a resonance), is *lowered* by 1.7 eV. This modification is a typical correlation effect of dielectric screening: Due to the polarizability of the

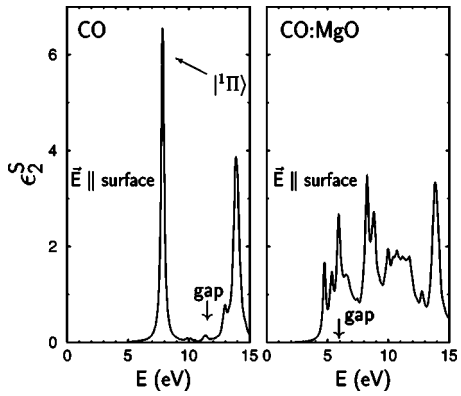

FIG. 7. Left panel: Optical absorption spectrum of the isolated CO monolayer, right panel: optical absorption spectrum of CO:MgO(100)–(1×1). A broadening of 0.14 eV is included in the figure.

substrate the Coulomb interaction inside the molecule is screened so that the self energy changes. Simply speaking, additional screening raises the positive correlation energy of the occupied levels and lowers the negative correlation energy of the empty states. Consequently the fundamental HOMO–LUMO gap closes.

C. Electron–hole excitations

The optical excitations of CO:MgO(001)–(1×1) are calculated from 22 occupied bands (i.e., 18 substrate and four molecular bands) and nine empty bands (i.e., six substrate bands and three molecular bands; cf. Table I). 36 **k** points in the two-dimensional surface Brillouin zone (SBZ) are sampled, which is consistent with the clean MgO surface. Figure 7 displays the resulting ϵ_2^S spectrum for the free-standing CO(001)–(1×1) film (left panel) and for the coupled CO:MgO(001)–(1×1) system.

The excitation spectrum of the free CO film is dominated by the $|^1\Pi\rangle$ state at an excitation energy of 7.9 eV, constituting the onset of molecular excitations. This state will be in the focus of our time-depending investigations below. The spectrum of the coupled system, on the other hand, is more complex. Its onset energy is 4.9 eV, given by two twofold degenerate exciton states with a binding energy of 1.2 eV. These states are charge-transfer excitons, i.e., they are formed from an electron on the molecules and a hole on the MgO substrate (see next paragraph). Due to the large variety of substrate hole orbitals, there is a large number of such charge-transfer states, covering the entire energy range from 4.9 to about 9 eV. In addition to these states, substrate-to-substrate excitations contribute to the spectrum above $\sim$7 eV, as well (cf. Sec. III B). It is important to note that the $|^1\Pi\rangle$ molecular state is not visible in the spectrum any more (see below).

The charge-transfer-exciton character of the excitations can be recognized in their wave function $\Psi_S(\mathbf{r}_e,\mathbf{r}_h)$ [see Eq. (7)]. To display Ψ_S, we calculate the exciton probability $|\Psi_S(\mathbf{r}_e,\mathbf{r}_h)|^2$ for a given hole position $\mathbf{r}_h$ and show the distribution of the electron relative to the hole, or vice versa.

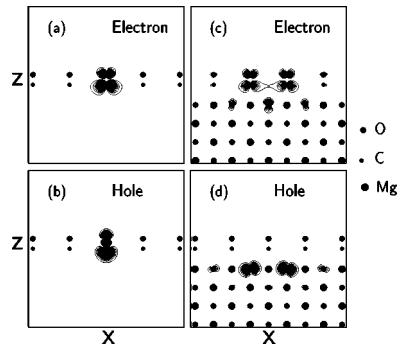

FIG. 8. Panels (a) and (b) show the distribution (side view) of the electron relative to the hole and the hole relative to the electron, respectively, for the first exciton state $|^1\Pi\rangle$ (at 7.9 eV) of the isolated CO monolayer. The hole in panel (a) and the electron in panel (b) are both located at the C atom. Panels (c) and (d) show the distribution (side view) of the electron relative to the hole and the hole relative to the electron, respectively, for the first exciton state (at 4.9 eV) of CO:MgO(001)–(1×1). The hole in panel (c) is located at the surface O atom and the electron in panel (d) is located at the C atom.

Note, that $\Psi_S(\mathbf{r}_e,\mathbf{r}_h)$ is periodic with respect to simultaneous lattice translation ($\mathbf{R}$) of both the electron ($\mathbf{r}_e$) and the hole ($\mathbf{r}_h$), i.e., $\Psi_S(\mathbf{r}_e,\mathbf{r}_h)=\Psi_S(\mathbf{r}_e+\mathbf{R},\mathbf{r}_h+\mathbf{R})$. On the other hand, the probability distribution of one of the particles relative to the other shows a spatial correlation which is *not* periodic.

Figure 8 shows such distributions for the lowest excited state of the free-standing CO film (i.e., the $|^1\Pi\rangle$ state; left panels) and for the lowest excited state (at 4.9 eV) of CO:MgO(001)–(1×1) (right panels). The upper (lower) panels display the electron (hole) distribution. In the case of the CO film, the respective other particle is located on the C atom of the central molecule. In the case of CO:MgO(001)–(1×1), the hole of panel (c) is located on the central atom of the substrate surface layer, and the electron of panel (d) is located on the central CO molecule. (Locating the hole on the molecule or the electron on the substrate gives very low amplitude for the state in question.) In the case of the $|^1\Pi\rangle$ molecular excitation (left side of Fig. 8, the hole and the electron are given by the CO 5σ and $2\pi^*$ orbitals, respectively. The lowest excitation of the coupled substrate–adsorbate system, on the other hand, has a completely different composition: The hole consists of O $2p_x/p_y$ orbitals in the MgO surface layer, while the electron is again given by the molecular $2\pi^*$ orbital. Note that, since the CO is located on top of a Mg atom, locating the hole on one surface O atom causes electron amplitude on several CO molecules [panel (c)], just as locating the electron on one molecule causes hole amplitude on several O surface atoms in panel (d). Similar distributions, i.e., the electron being on the molecules while the hole being distributed over substrate O atoms, is observed for most of the states in the excitation energy range of 5–9 eV, i.e., most of them are charge-transfer exciton states involving a transfer of the electron from the substrate to the molecule.

Since the nature of the charge-transfer excitons of the coupled system is so different from that of the molecular $|^1\Pi\rangle$ excitation, it is most interesting to investigate the be-

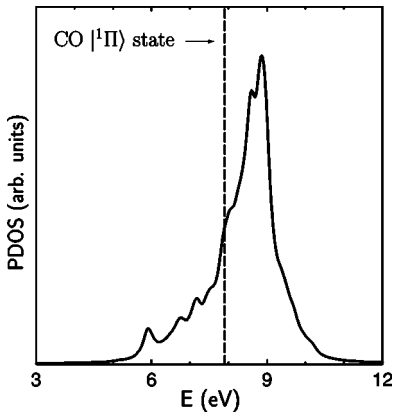

FIG. 9. Projected density of excitonic states $\Gamma(E)$ (solid curve) of the molecular $|^1\Pi\rangle$ state in the coupled CO:MgO(100)–(1×1) system. For comparison, the excitation energy of $|^1\Pi\rangle$ of the isolated CO monolayer (7.9 eV) is indicated by the dashed line.

havior of $|^1\Pi\rangle$ when it is coupled to the surface. If the state were not affected by the substrate, it should show up as a sharp line in the optical spectrum of CO:MgO(001)–(1×1), which is truly not the case (see right panel of Fig. 7). To analyze the effect of the substrate on $|^1\Pi\rangle$ in more detail, we define a projected density of excitonic states (PDOS) $\Gamma(E)$:

$$\Gamma(E) = \sum_S |\langle S|^1\Pi\rangle|^2 \delta(E - \Omega_S), \tag{14}$$

where $|S\rangle$ are all the eigenstates of Eq. (5) for the combined system CO:MgO(001)–(1×1), $|^1\Pi\rangle$ is the first exciton state (at 7.9 eV) of the isolated CO monolayer, and $\langle S|^1\Pi\rangle$ is the overlap between them.

This PDOS is displayed in Fig. 9. If $|^1\Pi\rangle$ were an eigenstate of the coupled CO:MgO system, the PDOS of Fig. 9 would be given by a sharp line. Instead, we observe a very broad curve around 8.9 eV, with a spectral width of more than 1 eV. Apparently, $|^1\Pi\rangle$ couples with many other states $|S\rangle$, most of which are charge-transfer states involving an electron on the molecule and a hole in the substrate.

We conclude from these results that the molecular state $|^1\Pi\rangle$ does not exist as an eigen state in the combined system CO:MgO(001)–(1×1). However, one can imagine that it might be prepared as an initial state of the free monolayer, before the interaction with the substrate is turned on at some time t_0. Since the state is then no longer an eigenstate, it will not persist as it is, but will rather develop into something different with time. We will discuss this time evolution in Sec. V.

V. TIME EVOLUTION OF ELECTRONIC EXCITATIONS

We now address the time propagation of the internal excitation of the molecule when it becomes coupled to the surface. This involves the dynamics of the $|^1\Pi\rangle$ state, as well as, the dynamics of individual charge carriers (electrons and holes) of which $|^1\Pi\rangle$ is composed.

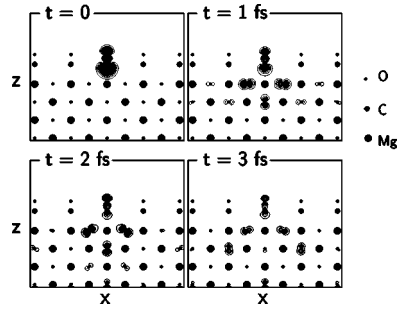

FIG. 10. Density distribution of the excited hole (starting from $|^1\Pi\rangle$) with increasing time for $\mathbf{r}_e$ at the central molecule. For better visibility, the charge density values in the substrate have been amplified by a factor of 5.

A. Dynamics of $|^1\Pi\rangle$

We construct $|^1\Pi\rangle$ in the free-standing (1×1) CO "film" (cf. left panel of Fig. 7) and consider this as the initial state of the Schrödinger equation of the coupled system, i.e., $\Psi(\mathbf{r}_e,\mathbf{r}_h,t=0)=\Psi^{(\mathrm{CO})}_{|^1\Pi\rangle}(\mathbf{r}_e,\mathbf{r}_h)$. The time propagation of the state and its wave function are then given by Eqs. (11) and (12). As illustration, Fig. 10 shows the spatial distribution of the hole with respect to the electron, and vice versa (cf. Fig. 8), at various times.

At $t=0$, the excitation is localized on the molecule by construction. At later times, the hole starts to hop to the O $2p$ orbitals of the substrate. Already after 1 fs a substantial amount of the hole amplitude has moved to the substrate surface layer. At still later times (e.g., $t=2$ fs or $t=3$ fs) the hole occupies more and more substrate space. Figure 10 also indicates that the transfer of the hole into the substrate does not only occur downwards but also laterally so that the "front line" resembles a spherical wave. Note that similar to the distributions shown in Fig. 8, the charge distributions are not periodic in space but rather show the correlation between the electron and hole.

In order to see how the exciton propagates along the vertical direction, we define a reduced correlation function between the z coordinates of the hole and the electron by $\chi(z_e,z_h,t)=\int|\Psi(\mathbf{r}_e,\mathbf{r}_h,t)|^2 dx_e dx_h dy_e dy_h$, i.e., by averaging the full electron-hole correlation function over the coordinates parallel to the surface. $\chi(z_e,z_h,t)$ thus gives the vertical distributions of the electron and the hole along the surface normal. Figure 11 shows $\chi(z_e,z_h,t)$ at various times. $z_e(z_h)$ denotes the vertical position of the excited electron (hole).

The two vertical and horizontal grid lines on the right and at the top indicate the z position of the atoms of the molecules, while the other grid lines indicate the atomic layers of the six-layer substrate slab. At $t=0$ the excitation is localized in the upper right corner by construction, i.e., both the electron and the hole are located in the molecular adlayer. Already after 1 fs, however, a significant portion of the hole has been transferred to the substrate. This transfer becomes even more pronounced after 2 fs when the hole amplitude on the molecule is already much smaller than that on the substrate layers. Note that after 3 fs the hole has reached the bottom of the slab, which might lead to reflection and interference be-

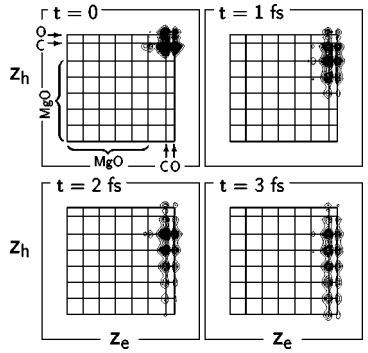

FIG. 11. Vertical electron-hole correlation function of the singlet excitation state (starting from $|^1\Pi\rangle$) with increasing time. $z_h(z_e)$ denote the vertical position of the excited hole (electron). The vertical and horizontal grid lines indicate the z position of the atoms of the CO molecule (on the right and at the top, respectively, of each panel), as well as the atomic layers of the six-layer substrate slab (on the left and at the bottom, respectively).

tween hole waves propagating downwards and upwards in z. Therefore, no definite conclusions about the propagation behavior beyond 3 fs are possible within the present supercell geometry containing six substrate layers (see discussion below).

Figure 11 clearly shows that only the hole transfers into the substrate while the electron remains on the molecule at all times. The reason for this behavior resides in the band structure shown in Fig. 6. Transfer of the electron from the molecular LUMO levels to the lower conduction bands of the substrate is not possible since the substrate bands are much higher in energy. Transfer of the *hole* from the molecular HOMO levels to the upper valence bands of the substrate, on the other hand, is possible. Due to this transfer the hole gains several eV of energy, which is used to break the strong electron–hole interaction (6 eV) inside the molecule. The electron–hole interaction of the charge-transfer excitons is much weaker (0.7–2.4 eV). The possibility to shift band-structure energy (gained by the transferred hole) into electron-hole interaction is the main reason why the excitation (i.e., the hole accompanied by the electron) can decay into substrate-related states. The transfer probability of a single hole from the molecule into the substrate, on the other hand, is much lower as we will show below.

B. Survival amplitude

A straightforward way of evaluating the transfer probability quantitatively is given by mapping the propagating state back onto the initial state, which constitutes a survival amplitude

$$A^{survival}_{|^1\Pi\rangle} = \langle \Psi(t=0)|\Psi(t)\rangle = \langle {}^1\Pi|\Psi(t)\rangle. \qquad (15)$$

The survival amplitude resulting from the system specifications used so far (six substrate layers, 36 **k** points) is shown in Fig. 12(a) by the dashed curve. As discussed above, systematic falsification of the time propagation may result after the hole has reached the lower surface of the slab. To address

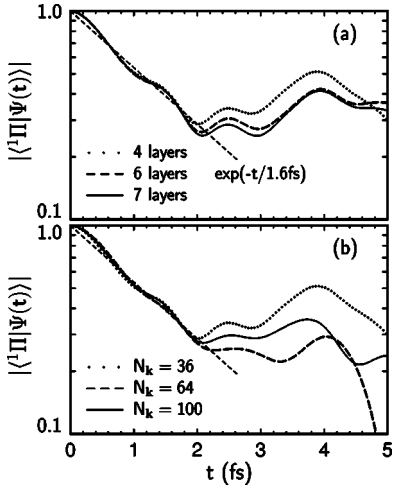

FIG. 12. Survival amplitude of the molecular excitation as a function of time (on a logarithmic scale). The three curves in panel a were calculated for the four-, six-, and seven-layer substrate slab, respectively, using 36 **k** points. The three curves in panel (b) were calculated for the four-layer substrate slab, using 36, 64, and 100 **k** points, respectively. The straight dashed line denotes a fit to the exponential decay as a guide to eye.

this, we have evaluated the time propagation in various systems, with the substrate thickness ranging from two to seven layers. Data for four, six, and seven layers are shown in Fig. 12(a). A second issue that might influence the survival amplitude relates to by the **k**-space representation of the excited states. A finite **k**-space sampling of the surface Brillouin zone by $n \times n$ grid points implies real-space repetition of the excited state with a periodicity of n surface lattice constants in each direction. Since the excited state broadens laterally in time (Fig. 10), it will mix with its replica after a certain time, which again might systematically falsify the survival amplitude. Furthermore, the coupling of the initial state $|^1\Pi\rangle$ with all other excited states $|S\rangle$ depends on the representation of $|S\rangle$ by the **k** point grid, as well. In order to investigate this, we have calculated the survival amplitude for the four-layer system using 36, 64, and 100 **k** points, respectively [see Fig. 12(b)].

All data show the following common features: (i) At early time ($t < 2$ fs) the survival amplitude drops very fast, reaching a value of about 0.3 at $t = 2$ fs. As a guide to the eye we include an exponential decay with a time constant of 1.6 fs, which may be interpreted as the (initial) lifetime of the decay process. (ii) Within the first 2 fs, the survival amplitude shows weak oscillations. These oscillations, i.e., the deviation from strictly exponential decay, are essentially the same for all layer thicknesses, and are also quite insensitive to the **k**-point resolution. (iii) After about $t = 2$ fs, the survival amplitude does no longer show a clear decaying behaviour, but exhibits some oscillations that depend sensitively on the substrate thickness and on the **k**-point sampling.

The fast initial decay within the first 2 fs can be understood from the discussion of Figs. 10 and 11, since the decaying survival amplitude simply reflects the transfer of the hole from the molecule to the substrate. The deviation from exponential decay, i.e., the weak oscillation within the first 2

fs, are more complex to analyze. Most importantly, note that a truly exponential decay cannot be expected. Exponential decay, as discussed within timedependent perturbation theory, results from the coupling of an initial state to a continuum of possible final states. In the present case, however, the coupling of $|^1\Pi\rangle$ is to the excited states $|S\rangle$ of the substrate–adsorbate system (in particular, the charge-transfer excitons), which do *not* form a true continuum. Instead, they form a discrete spectrum, as controlled by the attraction of the hole to the excited electron in the molecular adlayer and by the atomic structure of the substrate.

We have analyzed the survival amplitude until $t=100$ fs and observe that it remains well below 0.3 at all times, indicating that the separation of the hole from the electron on the molecule will persist. The most important observation of our study is that the very fast decay within the first 2 fs, having a decay time of $\sim$1.6 fs, is the same in all our calculations, thus constituting a stable and insensitive feature of the decay mechanism of the $|^1\Pi\rangle$ state. We note in passing that the $|^3\Pi\rangle$ triplet state behaves in a very similar way, with an even faster decay time of about 1.0 fs.

C. Details of the hole within $|^1\Pi\rangle$

The transfer of the hole can be analyzed in even more detail by averaging the vertical electron-hole correlation function $\chi(z_e,z_h,t)$ over z_e (the electron stays on the molecule anyway), thus arriving a z_h-dependent probability distribution for the hole only, changing with time:

$$\rho(z_h,t)=\int \chi(z_e,z_h,t)dz_e. \tag{16}$$

This quantity is shown in Fig. 13 for t between 0 and 4 fs (for the six-layer slab, using 36 **k** points).

At $t=0$, the hole is by construction localized at the CO molecule. There are three peaks surrounding the CO molecule, corresponding to the 5σ orbital of CO. The largest amplitude is between the C atom and the Mg substrate atom, i.e., slightly below the C atom. The outermost peak (slightly above the O atom of CO) has the second-largest amplitude, while the smallest peak is on the C–O bond. As the time increases from $t=0$ to $t=0.4$ fs, the first peak (below C) decreases while the third peak (above O) increases, i.e., the intramolecular charge distribution of the hole changes, shifting hole amplitude from the C atom towards the O atom. In addition, a small amount of the hole has already moved into the MgO surface layer. Since the survival amplitude measures (apart from the electron) the overlap of the hole distribution with the initial hole distribution, it is affected by both mechanisms (transfer towards the substrate and intramolecular redistribution). The intramolecular distribution of the hole continues to fluctuate at later times, as well, as can be seen in the changes of the relative amplitudes of the three intramolecular peaks, i.e., below C, above O, and between C and O. Between $t=0$ to $t=2$ fs, the peak below C decreases monotonically in time, while the peak above O does not change monotonically, i.e., the height ratio between the two peaks oscillates slightly, which may contribute to the deviation of the survival-amplitude decay from being strictly exponential.

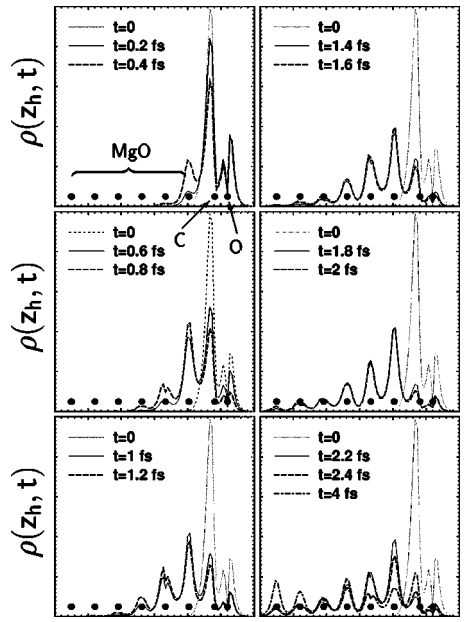

FIG. 13. Vertical density distribution $\rho(z_h,t)$ of the hole of the CO exciton for increasing time. As counting from the left to the right, the first six circles denote six atomic layers of the substrate and the last two solid circles denote the C atom sublayer and the O atom sublayer of the CO adlayer, respectively. For comparison, $\rho(z_h,t=0)$ is included in every panel.

Another feature concerns the amplitude of the molecular peak right below the C atom for times between 2 and 4 fs (see middle right and lower right panel of Fig. 13). Apparently, the amplitude of this peak *increases* after $t=2$ fs, i.e. some hole amplitude moves back from the substrate to the molecule. Therefore, $|\langle^1\Pi|\Psi(t)\rangle|$ for $t=2.4$ fs and $t=4$ fs is bigger than $|\langle^1\Pi|\Psi(t)\rangle|$ for $t=2$ fs, leading to the fluctuations of the small remnants of survival amplitude after $t=2$ fs (cf. Fig. 12). We note in passing that these features are again sensitive to the **k**-point sampling, leading to the quite different behavior of the survival amplitude after 2 fs.

D. Dynamics of single-particle excitations

As discussed above, the main reason why the excited hole can hop from the molecule into the substrate, although it is off-resonant with the substrate hole states, is due to the interaction with the simultaneously excited electron. Without the electron, the probability of hopping is much weaker. Only for holes in the 5σ orbital there is slight interaction with the substrate hole states, leading to the slight level repulsion (cf. the discussion of the band structure of Fig. 6) with the bottom of the valence bands. This interaction causes a small but nonzero hopping probability. To show this in detail, we discuss here the time propagation of the CO single-particle states after the molecule couples to the substrate. We use single-electron or single-hole states of the isolated CO monolayer as the initial state $\psi_{\mathbf{k}}(t=0)$ of the coupled system and then calculate $\psi_{\mathbf{k}}(t>0)$ using Eq. (13). To analyze the data, we evaluate again a survival amplitude of the states, i.e., the overlap with the initial state, $|\langle\psi_{\mathbf{k}}(t$

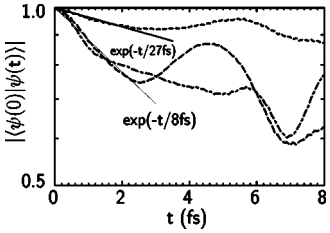

FIG. 14. Survival amplitude (on a logarithmic scale) of the CO 5σ single hole state at $\mathbf{k}=(0.4167,0.4167)2\pi/a$ (dashed-dotted curve), $\mathbf{k}=(0.5,0.4)2\pi/a$ (long dashed curve), and $\mathbf{k}=(0.5,0.45)2\pi/a$ (short dashed curve) in the coupled system containing six substrate atomic layers. As a guide to the eye, the thin and thick solid lines denote exponential decay with time constants of 8 and 27 fs, respectively.

$=0)|\psi_{\mathbf{k}}(t>0)\rangle|$ (which is now a scalar product between single-particle states instead of two-particle states). We have found that the CO electron states $2\pi^*$ and the CO hole states 4σ and 1π do not decay at all (for all $\mathbf{k}$ points) when the adlayer is coupled to the substrate. The only exceptions are CO 5σ hole states for wave vectors near the K point, at which the molecular band becomes slightly resonant with the substrate valence bands (see middle panel of Fig. 6), leading to some charge transfer into the substrate.

As representative examples, Fig. 14 shows the survival amplitude of the CO 5σ band for three wave vectors: $\mathbf{k}=(0.4167,0.4167)2\pi/a$, $\mathbf{k}=(0.5,0.4)2\pi/a$, and $\mathbf{k}=(0.5,0.45)2\pi/a$ ($a=2.98$ Å). Apparently, these states show a much slower decay (with typical decay constants of the order of 8–27 fs) than the decay of the exciton discussed above. This holds in particular for the hole state at the $\mathbf{k}$ point $(0.4167,0.4167)2\pi/a$, which is contained in the 36-$\mathbf{k}$-point representation of the exciton. This clearly shows that two-particle dynamics can be completely different from the dynamics of the contributing single particles and, in the present case, is much faster.

VI. CONCLUSIONS

We have used a combination of density-functional theory, many-body perturbation theory, and time-dependent quantum mechanics to reveal the time evolution of a molecular excitation coupled to a substrate. The system studied here is given by CO molecules adsorbed on the MgO(001)–(1×1) surface. It is characterized by a vertical adsorption geometry of the CO molecules on top of the Mg atoms with a Mg–C–O bonding configuration. As the most predominant molecular excitation, we have investigated the $|^1\Pi\rangle$ singlet-to-singlet transition, which occurs at an excitation energy of 7.9 eV. This molecular transition involves a hole in the 5σ state and an electron in the $2\pi^*$ state of the molecule. Both single-particle states are off-resonant with states of the MgO substrate and are thus long-lived single-particle states on their own, even though the molecule as a whole is coupled to the substrate. The $|^1\Pi\rangle$ state, however, although being composed from two such long-lived states, shows fast decay into substrate-related states with only a surprisingly small decay time of about 1.6 fs. A closer analysis reveals that the decay occurs into charge-transfer exciton states, composed from an electron on the molecule and a hole which is distributed over the substrate. The $|^1\Pi\rangle$ state thus undergoes a charge separation, i.e., the electron remains on the molecule while the hole is transferred into the MgO substrate. The decay time of 1.6 fs associated with this process is a factor of 5 shorter than the shortest decay time of single-particle processes between the molecule and the substrate.

ACKNOWLEDGMENTS

This work is financially supported by the Deutsche Forschungsgemeinschaft (Bonn, Germany) under Grant No. Ro 1318/4-1 and Ro 1318/5-1.

[1] H. Ferkel, J. T. Singleton, H. Reisler, and C. Wittig, Chem. Phys. Lett. **221**, 447 (1994); H. Ferkel, L. Hodgson, J. T. Singleton, P. M. Blass, H. Reisler, and C. Wittig, J. Chem. Phys. **100**, 9228 (1994).
[2] F. M. Zimmermann and W. Ho, Surf. Sci. Rep. **22**, 129 (1995).
[3] R. T. Jongma, G. Berden, D. van der Zande, T. Rasing, H. Zacharias, and G. Meijer, Phys. Rev. Lett. **78**, 1375 (1997).
[4] G. O. Sitz, Rep. Prog. Phys. **65**, 1165 (2002).
[5] A. G. Borisov, J. P. Gauyacq, E. V. Chulkov, V. M. Silkin, and P. M. Echenique, Phys. Rev. B **65**, 235434 (2002).
[6] S. Wright and E. Hasselbrink, J. Chem. Phys. **114**, 7228 (2001).
[7] C. Gahl, U. Bovensiepen, C. Frischkorn, and M. Wolf, Phys. Rev. Lett. **89**, 107402 (2002).
[8] Q. Zhong and M. Wolf, Surf. Sci. **496**, 21 (2002).
[9] N. P. Wang, M. Rohlfing, P. Krüger, and J. Pollmann, Phys. Rev. Lett. **92**, 216805 (2003).
[10] L. Hedin, Phys. Rev. **139**, A796 (1965).
[11] L. Hedin and S. Lundqvist, in *Solid State Physics, Advances in Research and Application*, edited by F. Seitz, D. Turnbull, and H. Ehrenreich (Academic, New York, 1969), Vol. 23, p. 1.
[12] M. S. Hybertsen and S. G. Louie, Phys. Rev. Lett. **55**, 1418 (1985); Phys. Rev. B **34**, 5390 (1986).
[13] W. Hanke and L. J. Sham, Phys. Rev. B **21**, 4656 (1980).
[14] G. Onida, L. Reining, R. W. Godby, R. Del Sole, and W. Andreoni, Phys. Rev. Lett. **75**, 818 (1995); S. Albrecht, L. Reining, R. Del Sole, and G. Onida, *ibid.* **80**, 4510 (1998).
[15] L. X. Benedict, E. L. Shirley, and R. B. Bohn, Phys. Rev. Lett. **80**, 4514 (1998); Phys. Rev. B **57**, R9385 (1998).
[16] M. Rohlfing and S. G. Louie, Phys. Rev. Lett. **80**, 3320 (1998); **81**, 2312 (1998); **82**, 1959 (1999); **83**, 856 (1999).
[17] M. Rohlfing and S. G. Louie, Phys. Rev. B **62**, 4927 (2000).
[18] G. Strinati, Phys. Rev. Lett. **49**, 1519 (1982); Phys. Rev. B **29**, 5718 (1984).
[19] J.-W. van der Horst, P. A. Bobbert, M. A. J. Michels, G. Brocks, and P. J. Kelly, Phys. Rev. Lett. **83**, 4413 (1999).
[20] J. C. Grossman, M. Rohlfing, L. Mitas, S. G. Louie, and M. L.

Cohen, Phys. Rev. Lett. **86**, 472 (2001)
[21] M. Rohlfing and S. G. Louie, Phys. Status Solidi A **175**, 17 (1999).
[22] P. H. Hahn, W. G. Schmidt, and F. Bechstedt, Phys. Rev. Lett. **88**, 016402 (2002).
[23] N. P. Wang, M. Rohlfing, P. Krüger, and J. Pollmann, Phys. Rev. B **67**, 115111 (2003).
[24] M. Rohlfing, N. P. Wang, P. Krüger, and J. Pollmann, Phys. Rev. Lett. **91**, 256802 (2003).
[25] E. A. Colbourn and W. C. Mackrodt, Surf. Sci. **143**, 391 (1984); R. Dovesi, R. Orlando, F. Ricca, and C. Roetti, *ibid.* **186**, 267 (1987); C. Pisani, R. Dovesi, R. Nada, and S. Tamiro, *ibid.* **216**, 489 (1989); K. M. Neyman and N. Rösch, *ibid.* **297**, 223 (1993).
[26] L. Chen, R. Wu, N. Kioussis, and Q. Zhang, Chem. Phys. Lett. **290**, 255 (1998);
[27] K. M. Neyman, S. P. Ruzankin, and N. Rösch, Chem. Phys. Lett. **246**, 546 (1995); T. A. Wesolowski, N. Vulliermet, and J. Weber, THEOCHEM **458**, 151 (1999); Y. Xu, J. Li, Y. Zhang, and W. Chen, Surf. Sci. **525**, 13 (2003);
[28] J. A. Snyder, D. R. Alfonso, J. E. Jaffe, Z. Lin, A. C. Hess, and M. Gutowski, J. Phys. Chem. B **104**, 4717 (2000).
[29] V. Panella, J. Suzanne, P. N. M. Hoang, and C. Girardet, J. Phys. I **4**, 905 (1994); P. N. M. Hoang, S. Picaud, and C. Girardet, Surf. Sci. **360**, 261 (1996); C. Girardet, P. N. M. Hoang, and S. Picaud, Phys. Rev. B **53**, 16 615 (1996).
[30] S. Furuyama, H. Fujii, M. Kawamura, and T. Morimota, J. Phys. Chem. **82**, 1028 (1978); E. A. Paccksht is, R. I. Soltanov, and N. E. Yurchenko, React. Kinet. Catal. Lett. **93**, 16 (1981); R. Wichtendahl, M. Rodriguez-Rodrigo, U. Hartel, H. Kuhlenbeck, and H. J. Freund, Surf. Sci. **423**, 90 (1999).
[31] C. R. Henry, C. Chapon, and C. Duriez, J. Chem. Phys. **95**, 700 (1991); J. W. He, C. A. Estrada, J. S. Corneille, M. C. Wu, and D. W. Goodman, Surf. Sci. **261**, 164 (1992);
[32] J. Fritsch, University of Regensburg (private communication).
[33] G. B. Bachelet, D. R. Hamann, and M. Schlüter, Phys. Rev. B **26**, 4199 (1982).
[34] M. Rohlfing, P. Krüger, and J. Pollmann, Phys. Rev. B **48**, 17 791 (1993); **52**, 1905 (1995).
[35] M. S. Hybertsen and S. G. Louie, Phys. Rev. B **37**, 2733 (1988).
[36] N. P. Wang, M. Rohlfing, R. Krüger, and J. Pollmann, Appl. Phys. A: Mater. Sci. Process. **78**, 213 (2004).
[37] R. C. Whited, C. J. Flaten, and W. C. Walker, Solid State Commun. **13**, 1903 (1973).
[38] E. Palik, *Handbook of Optical Constants of Solids* (Academic, New York, 1991), Vol. 11.
[39] K. Siegbahn, *ESCA Applied to Free Molecules* (North-Holland, Amsterdam, 1971).